Performance of missing transverse energy reconstruction in pp collisions at 13 TeV in the diphoton channel with ATLAS

S. Liao, B. Mellado and X. Ruan on behalf of the ATLAS Collaboration

School of Physics, University of the Witwatersrand, 1 Jan Smuts Avenue, Braamfontein, Johannesburg, 2000, South Africa

E-mail: shell-may.liao@cern.ch

Abstract. A good measurement of missing transverse energy is pre-eminent for many searches for new physics carried out by the ATLAS experiment at the LHC. The measurement of missing transverse energy in the ATLAS detector makes use of the full event reconstruction and a calibration based on reconstructed physics objects. The performance of MET reconstruction is evaluated using data collected in proton-proton collisions at a centre-of-mass energy of 13 TeV in Run 2 of data taking in the diphoton channel. Regrettably, these high luminosities achieved lead to undesirable backgrounds due to additional proton-proton collisions occurring at the same bunch crossing as the collision of interest (pile-up). As a result of this downside, several methods have been implemented in an effort to alleviate the effects of pile-up on the reconstruction and performance of MET. Some of these methods and the consequent performance of MET reconstruction at ATLAS in events with two photons are deliberated.

1. Introduction

A particle consistent with the Standard Model (SM) Higgs boson (h) was observed by the ATLAS [1] and CMS [2] collaborations back in 2012. Since then, more efforts have been directed towards performing Higgs boson measurements in order to better understand its properties. At the Large Hadron Collider (LHC), missing transverse energy (MET) plays an important role in Higgs boson measurements and various Beyond the Standard Model (BSM) physics searches. In proton-proton collisions most of the SM particles leave tracks or deposit energy inside the detector compartments as they traverse it, however, this is not the case for undetecteable particles such as neutrinos and other possible BSM particles. The initial momentum of the colliding particles is almost zero in the transverse plane such that the presence of these undetecteable particles can be inferred by the resultant momentum imbalance in this plane. This momentum imbalance is referred to as MET and is essentially enforced by energy-momentum conservation.

The high luminosity in Run 2 of data taking results in an increase in the additional proton-proton collisions which are superimposed on the hard physics processes. These additional interactions are referred to as pile-up interactions. MET measurement is significantly affected by these pile-up interactions and various techniques have been developed by ATLAS to suppress such effects. A high pile-up environment enhances the number of fake tracks thus increasing

the probability of misreconstruction. The performance of the reconstruction of this MET is therefore essential in evaluating these fake MET suppression efforts.

The diphoton channel ($h \to \gamma\gamma$) is important for searches for BSM physics, since new high-mass states decaying to two photons are predicted in many classes of extensions of the SM. The $h \to \gamma\gamma$ decay channel provides a very clean final-state topology with an invariant mass peak that is reconstructed with great precision. Final states in proton-proton collisions containing photons and significant MET emerge from a variety of new physics scenarios such as the search for dark matter (DM) in association with MET [3]. A hypothesized heavy scalar H is considered whereby $H \to h\chi\chi$, a search driven largely by MET such that $h(\to \gamma\gamma)$+MET. MET performance studies are essential for the search as well as other analyses in progress containing photons and MET signatures. This paper discusses MET performance studies in accordance with diphoton searches with MET signatures based on data recorded in 2015, 2016 and 2017 at a center-of-mass energy of 13 TeV. Altogether the data corresponds to 43.8 fb^{-1} of integrated luminosity.

2. The ATLAS detector

ATLAS is a multi-purpose particle detector with a forward-backward symmetric cylindrical geometry and a near 4π coverage in solid angle. It uses a right-handed coordinate system with the origin at the interaction point (IP) in the centre of the detector. The z-axis is along the beam pipe, the x-axis points from the IP to the centre of the LHC ring and the y-axis points upwards towards the earth's surface. In the transverse plane, cylindrical (r, ϕ) coordinates are used, where r is a radial dimension measuring the distance from the beam line and ϕ is the azimuthal angle around the beam pipe. The polar angle θ is the angle measured from the beam axis and the pseudorapidity is defined in terms of this angle as η = - ln[tan(θ/2)]. The pseudorapidity is used as an angular coordinate in place of θ and the angular separation between objects is defined as $\Delta R = \sqrt{\Delta\eta^2 + \Delta\phi^2}$. The transverse momentum, transverse energy and missing transverse momentum are all defined in the x-y plane.

ATLAS is made up of the following sub-systems: the inner detector (ID), the magnetic system, calorimeters and the Muon spectrometer (MS). The ID is surrounded by a 2 T superconducting solenoid which bends charged particles to enable particle momentum measurements. The ID tracks charged particles allowing particle identification and vertex measurements. This sub-system covers a pseudorapidity range of $|\eta| < 2.5$ [4]. The electromagnetic calorimeter (EMCAL) surrounds the ID and absorbs energy from particles which interact electromagnetically as they move through the detector. The EMCAL covers $|\eta| < 3.2$. The Hadronic calorimeter (HCAL) surrounds the EM calorimeter and is made up of steel plates and plastic scintillator plates which absorb energy from hadrons. These HCAL constituents provide a hadronic coverage of $|\eta| < 1.7$ and LAr technology is also used for the HCAL end-cap region. The entire HCAL covers a pseudorapidity range of $|\eta| < 4.9$. The outermost part of the detector is made up of the MS which consists of three large superconducting toroid systems which provide exceptional muon momentum measurements through accurate tracking.

3. MET reconstruction at ATLAS

MET is referred to as the energy which is not detected in a particle detector but is expected due to the laws of energy-momentum conservation. That is, the momentum in the transverse plane is expected to be zero implying that any vector momentum imbalance in the transverse plane goes into the MET calculation. MET is basically obtained from the negative vector sum of the momenta of all particles detected, these include: electrons, photons, hadronically decaying τ-leptons, jets and muons.

The electrons are reconstructed from energy deposits in the EMCAL, associated with tracks reconstructed in the ID. Those with $p_{\text{T}} > 10$ GeV and $|\eta| < 2.47$ are selected [5]. The photons

are reconstructed from energy clusters in the EMCAL and required to have $p_{\mathrm{T}} > 25\,\mathrm{GeV}$ and be within a region of $|\eta| < 2.3$. A *tight* photon identification requirement is applied to the photon candidates in order to reduce misidentification [6]. Hadronically decaying tau-leptons are required to have $p_{\mathrm{T}} > 20\,\mathrm{GeV}$ and be within $|\eta| < 2.5$ and those falling between $1.37 < |\eta| < 1.52$ are not considered. Muons are reconstructed from tracks in the ID and the MS and those with $p_{\mathrm{T}} > 10\,\mathrm{GeV}$ and $|\eta| < 2.7$ are selected. Muons in the region $|\eta| < 2.5$ must be matched to ID tracks. Jets are reconstructed from energy deposits in EMCAL and HCAL using the anti-kt algorithm [7]. They are required to have $p_{\mathrm{T}} > 20\,\mathrm{GeV}$ and be within $|\eta| < 4.5$. The jets with $|\eta| < 2.4$ and $p_{\mathrm{T}} < 60\,\mathrm{GeV}$ must pass the jet vertex tagger selection (JVT) [8]. This JVT technique separates hard scatter jets from pile-up jets in the central region of the detector, a very useful pile-up suppression method.

These physics objects are essentially the ingredients of the MET calculation which is done as follows [9, 10]:

$$E_{x(y)}^{miss} = E_{x(y)}^{miss,e} + E_{x(y)}^{miss,\gamma} + E_{x(y)}^{miss,\tau} + E_{x(y)}^{miss,jets} + E_{x(y)}^{miss,\mu} + E_{x(y)}^{miss,SoftTerm}, \tag{1}$$

where each term is calculated from the negative vectorial sum of momenta of the calibrated cell energies corresponding to objects as follows:

$$E_{x}^{miss,term} = -\sum_{i=1}^{N_{cell}^{term}} E_i sin\theta_i cos\phi_i \tag{2}$$

$$E_{y}^{miss,term} = -\sum_{i=1}^{N_{cell}^{term}} E_i sin\theta_i sin\phi_i \tag{3}$$

The actual value of MET (E_T^{miss}) and its azimuthal coordinate are calculated as follows:

$$E_T^{miss} = \sqrt{(E_x^{miss})^2 + (E_y^{miss})^2} \tag{4}$$

$$\phi^{miss} = \arctan\left(E_y^{miss}/E_x^{miss}\right) \tag{5}$$

Remaining calorimeter deposits not associated to the reconstructed objects are summed together in what is referred to as the *Soft Term* of equation 1. Several methods can be used to reconstruct the *Soft Term*, all of which affect the MET performance. At ATLAS the favourable method used to reconstruct the *Soft Term* is the track-based (TST) *Soft Term*.

ATLAS measures the momenta of charged particles using the ID and the series of hits in the ID which are efficiently reconstructed as tracks. Collisions which produce multiple tracks are reconstructed into vertices and these vertices give the position of the proton-proton collisions. Each vertex is required to have at least three tracks with $p_{\mathrm{T}} > 0.4\,\mathrm{GeV}$. The primary vertex (PV) in each event is selected as the vertex with the largest value of $\sum (p_{\mathrm{T}})^2$, where the scalar sum is taken over all the tracks associated to that particular vertex. The TST *Soft Term* is constructed from tracks passing these discussed selections with $p_{\mathrm{T}} > 0.5\,\mathrm{GeV}$ and not associated to any of the hard physics objects. This method allows excellent vertex association of the *Soft Term* used in the MET reconstruction.

4. MET performance

This section shows some basic MET distributions after the diphoton selection. In the $h \to \gamma\gamma$ final state at least two photon candidates are required such that the leading photon has $p_{\mathrm{T}} > 35\,\mathrm{GeV}$ and the sub-leading has $p_{\mathrm{T}} > 25\,\mathrm{GeV}$. Following this, in order to maintain good data quality, the events passing this selection pass through additional selection criteria. As

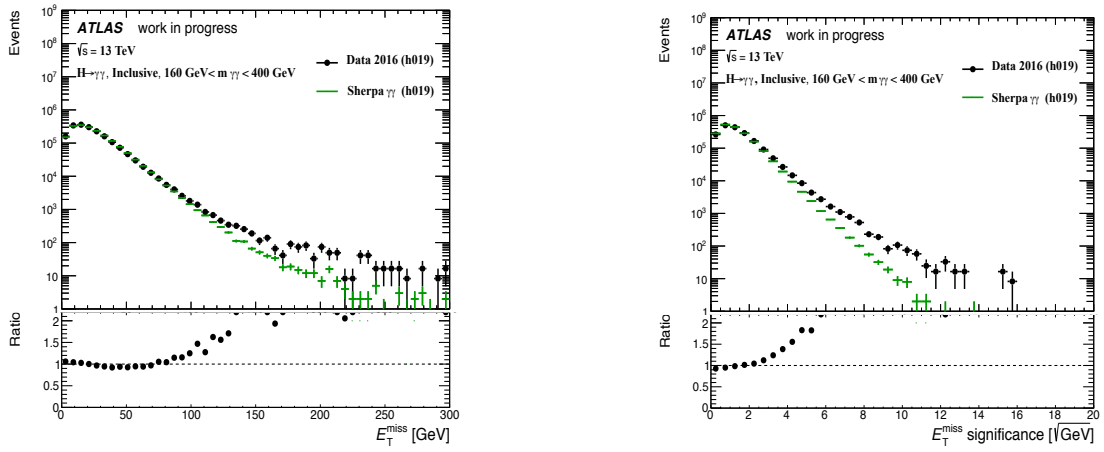

(a) **(b)**

Figure 1: MET TST distributions comparing 2015+2016 data corresponding to 36.1 fb^{-1} and Sherpa $\gamma\gamma$ MC, where (a) is the MET distribution and (b) is the MET significance distribution. The MC has been normalized to the total number of events in the inclusive sample of the data [11].

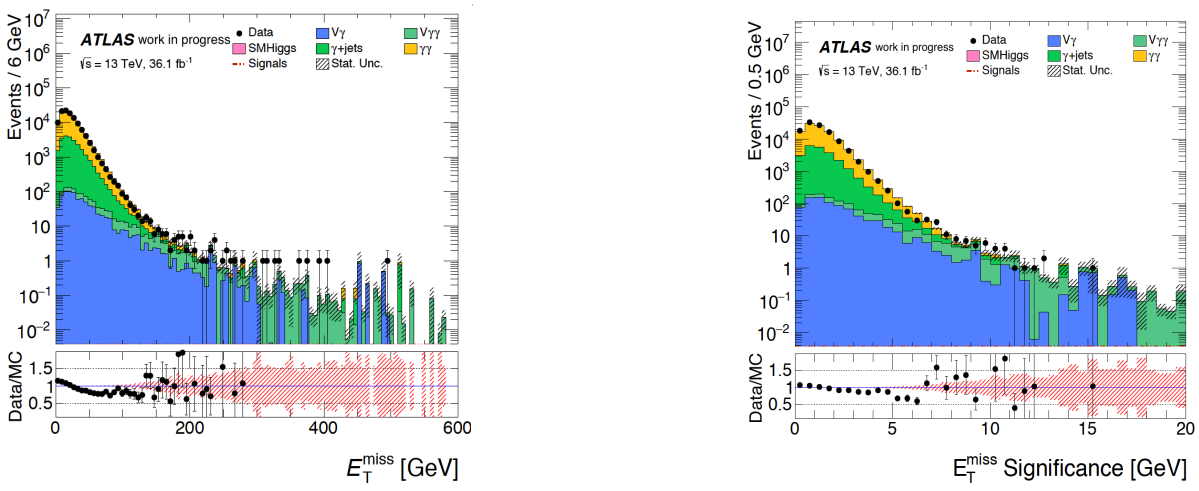

(a) **(b)**

Figure 2: MET TST distributions comparing 2015+2016 data corresponding to 36.1 fb^{-1} and additional processes, where (a) is the MET distribution and (b) is the MET significance distribution. The MC have been normalized to the total number of events in the inclusive sample of the data [11].

discussed in Section 3, the photon candidates must satisfy *tight* ID criteria and satisfy the following relative p_{T} cuts: leading must satisfy $p_{\mathrm{T}_{\gamma 1}}/m_{\gamma\gamma} > 0.35$ and sub-leading must satisfy $p_{\mathrm{T}_{\gamma 2}}/m_{\gamma\gamma} > 0.25$. Lastly, the events are required to have 160 GeV $< m_{\gamma\gamma} <$ 400 GeV where the diphoton mass is calculated assuming that the photons originate from the diphoton primary vertex. The diphoton primary vertex position is obtained by combining the trajectories of both photon candidates.

The performance checks are done using 2015+2016 data corresponding to 36.1 fb^{-1} and 2015+2016+2017 data corresponding to 43.8 fb^{-1}, respectively. The Higgs boson signal Monte Carlo (MC) comprises the ggF, VBF, Wh, Zh and $t\bar{t}h$ production modes. The signals produced via ggF and VBF are generated with `PowHeg` [12]. The Wh and Zh are generated with

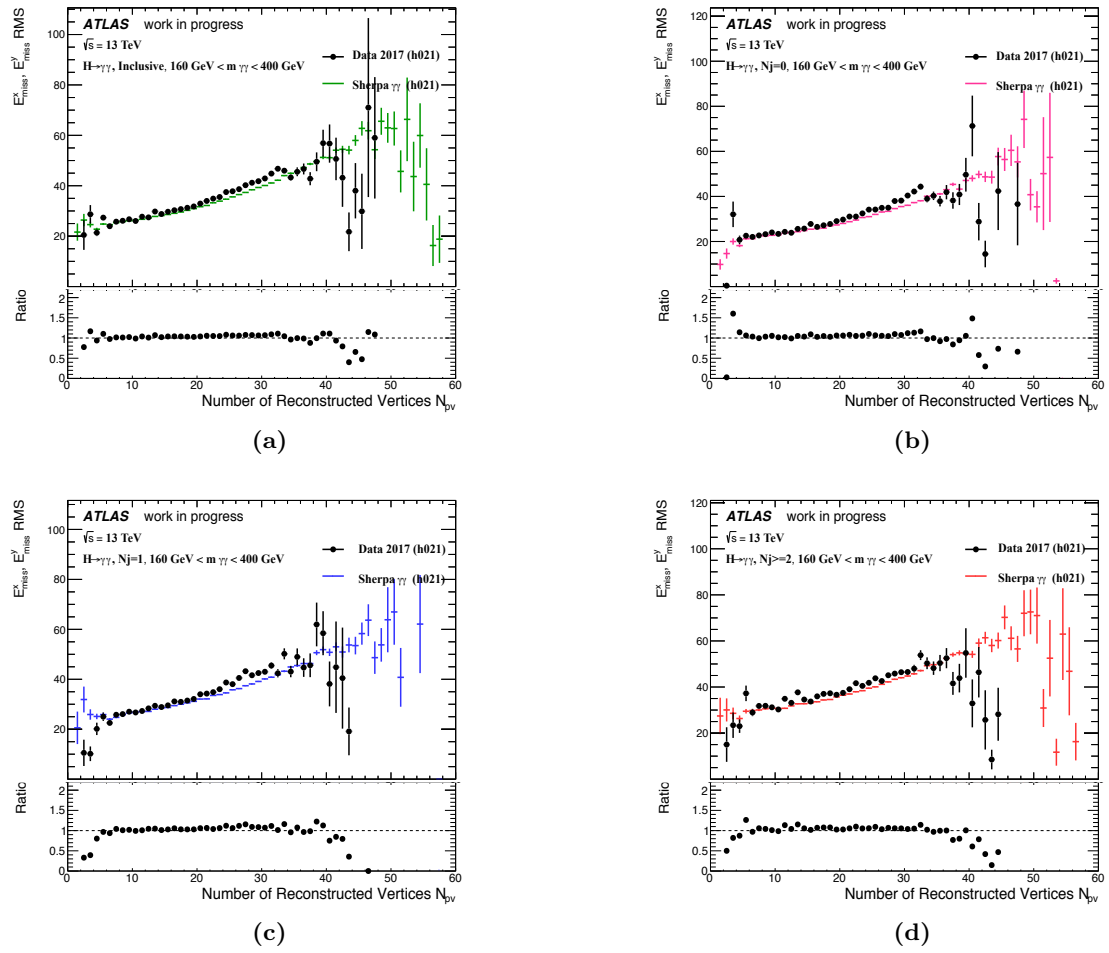

Figure 3: $E_{\mathrm{T}}^{\mathrm{miss}}$ resolution distributions showing the x and y components of the $E_{\mathrm{T}}^{\mathrm{miss}}$ as a function of N_{pv}. The comparisons are between 2015+2016+2017 data corresponding to 43.8 fb^{-1} and Sherpa $\gamma\gamma$ MC. The distributions are split into (a) inclusive case, (b) 0-jet case, (c) 1-jet case and (d) $\geq$2-jet case [11].

`Pythia8` [13] and the $t\bar{t}h$ signal is generated with `MadGraph5` aMC@NLO [14]. For the direct comparison checks, the Sherpa $\gamma\gamma$ MC is used as this is the most dominant background. The Sherpa $\gamma\gamma$ events are simulated using the `SHERPA` version 2.1 event generator [15] with up to two additional partons in the final state with the CT10 PDF. `SHERPA` is also used to genarate $V\gamma$ and $V\gamma\gamma$ backgrounds which are also contributors. The γ+jets background sample is represented by data, whereby only one of the two photons in the selection is required to pass the reverse photon isolation criteria.

Figure 1 shows the data versus Sherpa $\gamma\gamma$ MC while Figure 2 shows the data versus additional MC [11]. Figure 1(a) respresents the MET TST distribution and Figure 1(b) shows MET TST significance distribution and in both cases MC has been normalized to the total number of events in the inclusive sample of the data. Some discrepancies are observed in the tails of these distributions. These are reduced by the addition of other processes with real MET as can be seen in Figure 2. Good agreement is then observed between data and MC with the addition of other processes.

In order to study the degradation of the MET performance the MET resolution distributions

are of great importance. The resolution distributions shown are done using 2015+2016+2017 blinded data corresponding to 43.8 fb^{-1} of integrated luminosity. The root-mean-square (RMS) of the superimposed x and y components of the $E_{\text{T}}^{\text{miss}}$ is used to estimate the resolution. Figure 3 shows the MET resolution as a function of the number of primary vertices (N_{pv}) for the Figure 3(a) inclusive case, Figure 3(b) 0-jet case, Figure 3(c) 1-jet case and Figure 3(d) $\geq$2-jet case. Good agreements are observed. The most stable performance is observed in the case where no jets (0-jet) are required as it has the least slope. In fact, all the jet binning cases perform better than the inclusive case which has the highest slope. This shows that an increased number of jets degrades the MET resolution.

5. Conclusion

The measurement of MET is an important attribute of numerous interesting physics analyses at the LHC. The ATLAS calorimeter provides commendable energy resolution but is highly sensitive to pile-up. The reconstruction and performance of MET based on various recent datasets and MC has been presented. The reconstructed MET is validated using Run 2 ATLAS data showing a good agreement with Monte Carlo simulation. MET resolution distributions have been studied by binning in jet multiplicity in order to observe the effects of the presence of jets on the MET performance. Looking at the jet binning cases it is clear that the degradation in resolution originates mostly from the jet multiplicity and thus the amount of overall activity within the detector. In fact, the resolution in the inclusive case has a slightly larger slope than the jet binning cases, which implies that the higher slope comes from an increased number of jets at larger N_{pv}.

Acknowledgements

I would like to thank the SA-CERN program for providing the research opportunity to visit CERN. The National Research Foundation (NRF) of South Africa for the bursary they provided. I would also like to thank the School of Physics, the Faculty of Science and the Research Office at the University of the Witwatersrand.

References

[1] Aad G *et al.* (ATLAS) 2012 *Physics Letters B* **716** 1–29 ISSN 03702693 (*Preprint* 1207.7214)
[2] Khachatryan V *et al.* (CMS) 2012 *Physics Letters B* **716** 30–61 ISSN 03702693 (*Preprint* 1207.7235)
[3] Aad G *et al.* (ATLAS) 2017 *Phys. Rev. Lett.* **119** 181804 (*Preprint* 1707.01302)
[4] Aad G *et al.* (ATLAS) 2012 *The European Physical Journal C* **72** 1844 ISSN 1434-6044 (*Preprint* 1108.5602)
[5] Aad G *et al.* (ATLAS) 2014 *Eur. Phys. J.* **C74** 3071 (*Preprint* 1407.5063)
[6] Aad G *et al.* (ATLAS) 2016 *Eur. Phys. J.* **C76** 666 (*Preprint* 1606.01813)
[7] Cacciari M, Salam G P and Soyez G 2008 *JHEP* **04** 063 (*Preprint* 0802.1189)
[8] Aad G *et al.* (ATLAS) 2014 Tagging and suppression of pileup jets with the ATLAS detector Tech. Rep. ATLAS-CONF-2014-018 Geneva URL https://cds.cern.ch/record/1700870
[9] Aad G *et al.* (ATLAS) 2012 *Eur. Phys. J.* **C72** 1844 (*Preprint* 1108.5602)
[10] Aad G *et al.* 2015 Performance of missing transverse momentum reconstruction for the ATLAS detector in the first proton-proton collisions at at $\sqrt{s}$= 13 TeV Tech. Rep. ATL-PHYS-PUB-2015-027 CERN Geneva URL https://cds.cern.ch/record/2037904
[11] Ruan X *et al.* 2018 Supporting note: Search for a new resonance in the di-photon decay in association with missing transverse energy in pp collisions at $\sqrt{s}$ = 13 TeV with the ATLAS detector Tech. Rep. ATL-COM-PHYS-2018-970 CERN Geneva URL https://cds.cern.ch/record/2628349
[12] Nason P and Oleari C 2010 *JHEP* **02** 037 (*Preprint* 0911.5299)
[13] Sjostrand T, Mrenna S and Skands P Z 2008 *Comput. Phys. Commun.* **178** 852–867 (*Preprint* 0710.3820)
[14] Alwall J, Frederix R, Frixione S, Hirschi V, Maltoni F, Mattelaer O, Shao H S, Stelzer T, Torrielli P and Zaro M 2014 *JHEP* **07** 079 (*Preprint* 1405.0301)
[15] Gleisberg T, Hoeche S, Krauss F, Schonherr M, Schumann S, Siegert F and Winter J 2009 *JHEP* **02** 007 (*Preprint* 0811.4622)